Solar partitioning in a changing Arctic sea-ice cover

D.K. PEROVICH,[1] K.F. JONES,[1] B. LIGHT,[2] H. EICKEN,[3] T. MARKUS,[4] J. STROEVE,[5] R. LINDSAY[2]

[1]*US Army Engineer Research and Development Center, Cold Regions Research and Engineering Laboratory, 72 Lyme Road, Hanover, NH 03755-1290, USA*
E-mail: donald.k.perovich@usace.army.mil
[2]*Polar Science Center, Applied Physics Laboratory, University of Washington, 1013 NE 40th Street, Seattle, WA 98105-6698, USA*
[3]*Geophysical Institute, University of Alaska Fairbanks, PO Box 757320, Fairbanks, AK 99775-7320, USA*
[4]*NASA Goddard Space Flight Center, Code 614.1, Greenbelt, MD 20771, USA*
[5]*National Snow and Ice Data Center, University of Colorado, 1540 30th Street, Boulder, CO 80309-0449, USA*

ABSTRACT. The summer extent of the Arctic sea-ice cover has decreased in recent decades and there have been alterations in the timing and duration of the summer melt season. These changes in ice conditions have affected the partitioning of solar radiation in the Arctic atmosphere–ice–ocean system. The impact of sea-ice changes on solar partitioning is examined on a pan-Arctic scale using a 25 km × 25 km Equal-Area Scalable Earth Grid for the years 1979–2007. Daily values of incident solar irradiance are obtained from NCEP reanalysis products adjusted by ERA-40, and ice concentrations are determined from passive microwave satellite data. The albedo of the ice is parameterized by a five-stage process that includes dry snow, melting snow, melt pond formation, melt pond evolution, and freeze-up. The timing of these stages is governed by the onset dates of summer melt and fall freeze-up, which are determined from satellite observations. Trends of solar heat input to the ice were mixed, with increases due to longer melt seasons and decreases due to reduced ice concentration. Results indicate a general trend of increasing solar heat input to the Arctic ice–ocean system due to declines in albedo induced by decreases in ice concentration and longer melt seasons. The evolution of sea-ice albedo, and hence the total solar heating of the ice–ocean system, is more sensitive to the date of melt onset than the date of fall freeze-up. The largest increases in total annual solar heat input from 1979 to 2007, averaging as much as 4% a^{-1}, occurred in the Chukchi Sea region. The contribution of solar heat to the ocean is increasing faster than the contribution to the ice due to the loss of sea ice.

INTRODUCTION

There has been a pronounced decrease in the summer Arctic sea-ice cover over the past decade. September ice extent has declined at an average rate of 11% $(10\,a)^{-1}$ (Serreze and others, 2007; Comiso and others, 2008; Stroeve and others, 2008). Observations from submarines, aircraft and satellites indicate that ice thickness is also decreasing (Giles and others, 2008; Haas and others, 2008; Rothrock and others, 2008; Kwok and others, 2009). The ice cover has transitioned to a younger, thinner, more vulnerable state (Maslanik and others, 2007; Nghiem and others, 2007). There has been considerable research examining the influence of atmospheric and oceanic forcing on the observed decline in sea ice. Contributions to the ice decline include a general overall warming trend (Richter-Menge, 2009), variations in cloudiness (Francis and Hunter, 2006; Kay and others, 2008), shifts in atmospheric circulation patterns (Rigor and Wallace, 2004), increased ice export from the Fram Strait (Nghiem and others, 2007), advected ocean heat from lower latitudes (Shimada and others, 2006; Woodgate and others, 2006; Polyakov and others, 2007), increased solar heating of the upper ocean (Perovich and others, 2007a, 2008; Steele and others, 2008) and increases in the length of the melt season (Markus and others, 2009).

In this paper, we focus on the impact that increases in melt season length have on ice albedo and solar heat input to the ice (Perovich, and others, 2007b). The impact of solar heat on the ice–ocean system is at the core of the ice-albedo feedback. Perovich and others (2007a) examined changes in the solar heating of open water in the Arctic Ocean and adjacent seas. Here we take a similar approach, but with a focus on examining the role of solar heating of the ice. A simple parameterization of ice albedo, based on field observations (Perovich and others, 2002) and triggered by the onset of melt and freeze-up is used (Markus and others, 2009). Averages and trends in solar heat input to the ice cover over the period 1979–2007 are computed and compared to values for the solar heat input to the ocean.

METHODS

The flux of solar heat input to the ice–ocean system (F_{in}) is simply the flux of solar heat input to the ice (F_i) and to the ocean (F_o) and can be expressed as

$$F_{in} = F_i + F_o.$$

Expanding gives

$$F_{in}(t) = F_r(t)C(t)[1 - \alpha_i(t)] + F_r(t)[1 - C(t)](1 - \alpha_o), \quad (1)$$

where F_r is the incident solar irradiance, C is the ice concentration, α_i is the ice albedo, α_o is the ocean albedo and t is time, indicating which variables are a function of time. It is assumed that no sunlight penetrates the ice into the ocean. Perovich and others (2007a) examined the F_o term and here we concentrate on evaluating F_i. Equation (1) was evaluated daily from 1979 to 2007 on a 25 km × 25 km

https://doi.org/10.3189/172756411795931543 Published online by Cambridge University Press

Equal-Area Scalable Earth Grid. Four parameters are needed for this calculation: $F_r(t)$, $C(t)$, α_o and $\alpha_i(t)$.

The mean daily downwelling shortwave fluxes from the US National Centers for Environmental Prediction (NCEP) reanalysis are known to have large biases due to incorrect cloud fractions compared to those of the European Centre for Medium-Range Weather Forecasts reanalysis (ERA-40) (Serreze and others, 1998; Walsh and others, 2009). Walsh and others (2009) find that at the Barrow (Alaska) ARM (US Atmospheric Radiation Measurement Program) site, shortwave flux biases averaged over June–August for ERA-40 are 16 W m^{-2} too high compared to 143 W m^{-2} too high for the NCEP reanalyses. The NCEP bias results from simulated summertime cloud fractions that are too small. The ERA-40 reanalysis has a more realistic seasonal cycle for clouds, but the data end in 2002. The fluxes in the two reanalyses are well correlated if seasonal and geographic variations are accounted for (Liu and others, 2005), so we can utilize the more accurate ERA-40 values to correct the post-2002 NCEP data by determining seasonal and regional regression equations between the two datasets

The NCEP predictor variables are the downwelling solar flux, $F_{swd,\ ncep}$, and the sea-level pressure, P_{ncep}. These are the two variables we found that significantly improved the NCEP estimates. The ERA-40 downwelling solar flux was interpolated to the NCEP grid using five years of data, evenly spaced from 1979 to 1999. Separate regression equations were determined every 5 days of the seasonal cycle for every second gridpoint of the NCEP data. This is justified because the regression coefficients do not change rapidly with the seasonal cycle or location. All pairs (NCEP and ERA-40) of daily average values were included for each fit within 5 days of the designated time of year from all five years and within 750 km of the grid location. For location, x, and time of season, s, the least-squares estimates of the coefficients were determined for

$$F_{swd,\,era-40} = a_0(x,s) + a_1(x,s)F_{swd,\,ncep} + a_2(x,s)P_{ncep}.$$

The mean root-mean-square error of the regression is 29 W m^{-2}. Biases in the ERA-40 downwelling shortwave flux remain in the adjusted data. Finally, corrected estimates of the daily mean solar flux were computed for all locations and times on the NCEP grid by interpolating the three coefficients to each time and location and using the NCEP values for the downwelling solar flux and the sea-level pressure in the regression equation.

Passive microwave observations were used to determine the ice concentration, $C(t)$, from the NASA Team algorithm (J. Maslanik and J. Stroeve, http://nsidc.org/data/docs/daac/nsidc0081_ssmi_nrt_seaice.gd.html; D. Cavalieri and others, http://nsidc.org/data/nsidc-0051.html). Summer melt ponds may lead to underestimates of ice concentration, due to the difficulty in distinguishing between ponds and leads. We do not expect there to be any temporal trend in this uncertainty. Based on the field observations of Pegau and Paulson (2001) the albedo of the open ocean was set to a constant 0.07, with no time dependence.

The most difficult time series to estimate was the ice albedo. Due to persistent summer clouds, there is a not a comprehensive dataset of remotely sensed sea-ice albedos. The evolution of sea-ice albedo was approximated from the field observations of Perovich and others (2002). They determined that the seasonal evolution of albedo for multi-year ice has five distinct stages, namely, dry snow, melting snow, melt pond formation, melt pond evolution, and fall freeze-up, and that the evolutionary sequence is determined in large part by the onset dates of melt and freeze-up. This albedo sequence is applied everywhere in our region of interest, but the daily values of albedo depend on the local onset dates of melt and freeze-up. The albedo sequence includes melt ponds, assuming they follow an evolution similar to that observed by Perovich and others (2002). Using the method of Markus and others (2009), daily-averaged satellite passive microwave temperatures are used to map four onset dates for each gridcell for each year: early melt, full melt, early freeze-up and full freeze-up. Briefly, the melt season is determined using temporal changes in brightness temperatures at 37 GHz and temporal changes in the gradient ratio between 19 and 37 GHz. The melt indicator of Smith (1998) is also applied. The strength of all three indicators determines the beginning and end of the period of continuous melt. The first and last days of melt are identified by secondary peaks in the weight of the three indicators before and after the melt starts and ends. Finally, sea-ice concentration provides additional information on ice disintegration and formation. Using the four melt/freeze-up dates the following sequence in albedo evolution is applied at all gridcells for all years:

1. Before melt onset the snow albedo is 0.85.
2. At early melt the albedo decreases to 0.81.
3. Starting with full melt, there is a linear decrease to 0.71 in 15 days.
4. For the next 6 days, decrease from 0.70 to 0.50.
5. Albedo decreases by 0.0029 d^{-1} (but to no less than 0.2).
6. At early freeze-up set albedo to 0.46, representing some ponds freezing.
7. At full freeze-up, albedo increases by 0.026 d^{-1} to 0.85.

Applying this algorithm, with the satellite-derived onset dates, we were able to evaluate Equation (1) at all grid locations every day from 1979 to 2007. The resulting solar flux was then integrated over time to compute the total annual solar heat input to the ice. This is done by calculating the solar heat input to the ice per unit area for the entire gridcell,

$$Q_i = \sum F_r(t)C(t)[1 - \alpha_i(t)]\Delta t,$$

where Δt is 1 day (86 400 s) and the summation is over all days of the year. If no ice is present in a gridcell ($C = 0$), then there is no contribution to Q_i for that day. Similarly the solar heat input directly to the ocean, Q_o, per unit area for the entire gridcell is

$$Q_o = \sum F_r(t)[1 - C(t)][1 - \alpha_o(t)]\Delta t.$$

The mean annual values of Q_o and Q_i are computed for the period 1979–2007, and year-to-year trends over that period are calculated. The relative contributions of solar heat deposited in the ice and in the ocean are explored.

RESULTS

The mean annual solar heat input to the ice for 1979–2007 is mapped in Figure 1. Mean values range from 100 to 1000 MJ m^{-2}. The minimum solar heat input to the ice occurs at the edge of the marginal ice zone in the

https://doi.org/10.3189/172756411795931543 Published online by Cambridge University Press

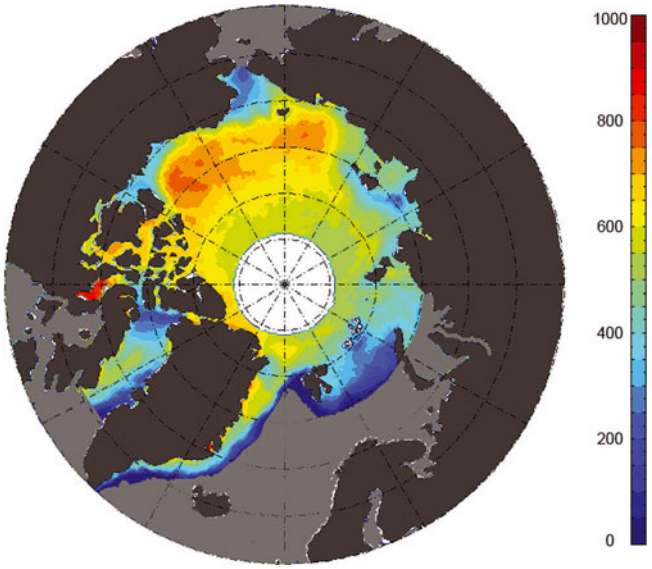

Fig. 1. Mean value of total annual solar heat input to the ice within a gridcell, Q_i. The units are MJ m^{-2}.

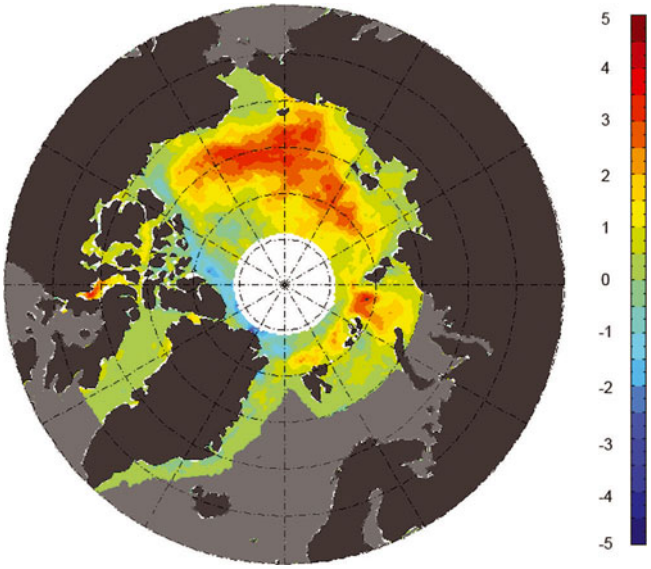

Fig. 3. The trend of the relative contribution of solar heat deposited in open water to the total solar heat deposited in the ice–ocean system, $Q_o/(Q_o + Q_i)$. The units are % a^{-1}.

Greenland Sea, where ocean heat drives the spring ice retreat, before much solar heat is absorbed in the ice. In contrast, peak solar heating occurs in the eastern Beaufort Sea where incident solar radiation is large, surface melting starts early and the albedo is small. In the Arctic basin, solar heating of the ice decreases northward from about 700 to 500 MJ m^{-2} due to reduced incident solar irradiance and a shorter melt season.

To put these numbers in perspective, it takes ~300 MJ m^{-2} to thin the ice by 1 m. Of course all the solar heat deposited does not contribute to surface melting; some is absorbed in the interior of the ice and some is transmitted to the ocean. Also, there are other major components to the surface heat budget (e.g. longwave radiative losses) that temper the impact of solar heating.

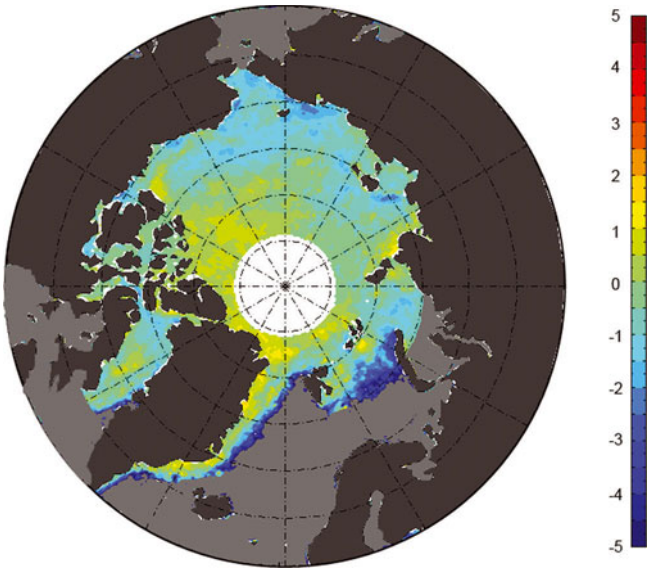

Fig. 2. The trend in total annual solar heat input to the ice within a gridcell, Q_i. The units are % a^{-1}.

The 1979–2007 trend in solar heat input to the ice is mapped in Figure 2. This was calculated by performing a linear least-squares fit to the time series of annual Q_i for each gridcell. Trends are generally modest and are a mix of positive and negative values. This mix is a result of the two distinct parameters that contribute to Q_i: the ice concentration and the ice albedo. The negative trends around the periphery of the Arctic are due to reductions in ice concentration. The strongest negative trends are mainly near Greenland and the Fram Strait and result from ice completely melting earlier in the season, so that solar heat goes into the ocean rather than the ice. Areas of positive trend in Q_i are regions where ice concentration has not changed appreciably over the years, but the melt seasons have lengthened, resulting in an overall decrease in albedo.

Figure 3 explores trends in the relative contribution of solar heat input to open water compared to the entire gridcell, by plotting the trend of the ratio $Q_o/(Q_o + Q_i)$. Roughly 90% of the study area shows an increasing relative contribution from solar heat absorbed in open water, averaging 1% a^{-1}, with a peak of 4% a^{-1}. The growth in the open-water solar heat contribution is primarily due to a trend of increasing open water.

Longer melt seasons have resulted in modest increases in solar heating of the ice. This results in some increases in surface melting, but the impact is likely moderated by other components of the surface heat budget (Perovich and others, 2010). However, in interpreting Figure 2, it needs to be kept in mind that our simplified approach does not account for the replacement of multi-year ice by first-year ice with lower summer albedos (Perovich and others, 2002). The contribution of solar heat to the ocean is increasing faster than the contribution to the ice due to the loss of sea ice. This impacts the sea-ice mass balance through a trend of increasing bottom melt (Maykut and McPhee, 1995; Perovich and others, 2008) or reduced ice formation in the fall and winter. Extra heat deposited in leads also increases lateral melting of floes. Lateral melt is a

https://doi.org/10.3189/172756411795931543 Published online by Cambridge University Press

major mechanism for the ice-albedo feedback because as the area of open water is increased the mean albedo is reduced. Determining the degree of this enhancement requires further research.

DISCUSSION

The analysis in this paper is a first step in assessing changes in solar heat input to the ice as a result of changes in the melt season. The impact of increasing seasonal ice replacing multi-year ice should be considered next. This entails distinguishing between multi-year and first-year ice, using both passive and active microwave sensors, and then applying an appropriate albedo evolution algorithm to each type. An algorithm for the albedo evolution of first-year ice needs to be developed to complement the multi-year ice algorithm that was applied here. Field observations indicate that first-year ice has a somewhat similar, but amplified, albedo evolution compared to multi-year ice. There are significant differences as well. First-year ice typically has a thinner snow cover than multi-year ice, so the melt of the snow cover is faster and pond formation occurs earlier. Due to its flat topography, pond fractions early in the pond formation stage can be as large as 90%, much greater than multi-year ice. After drainage occurs in the pond evolution stage, first-year pond fractions are closer to multi-year ice values (Hanesiak and others, 2001; Grenfell and Perovich, 2004). There is a rapid decrease in bare ice albedo if the ice thickness drops below ~0.5–0.7 m. Should the first-year ice completely melt in summer, the fall freeze-up of open water will take much longer than it does in an area with multi-year ice. Taken together this implies that albedos for first-year ice are less than those for multi-year ice over the course of the melt season, and the solar heat input to the ice is significantly greater. Our analysis applying a multi-year ice albedo evolution algorithm to seasonal ice overestimates the albedo and thus underestimates the solar heat input. As the multi-year ice pack declines and more of the Arctic has a seasonal ice cover, more solar heat will be input to the ice–ocean system, resulting in an enhanced ice-albedo feedback.

ACKNOWLEDGEMENTS

This work has been funded by the US National Science Foundation Arctic System Science Program and the NASA Cryospheric Program. The work on melt/freeze-up dates was funded under NASA Award No. NNG04GO51G. We appreciate the efforts of the reviewers and the scientific editor in improving the manuscript.

REFERENCES

Comiso, J.C., C.L. Parkinson, R. Gersten and L. Stock. 2008. Accelerated decline in the Arctic sea ice cover. *Geophys. Res. Lett.,* **35**(1), L01703. (10.1029/2007GL031972.)

Francis, J.A. and E. Hunter. 2006. New insight into the disappearing Arctic sea ice. *Eos,* **87**(46), 509.

Giles, K.A., S.W. Laxon and A.L. Ridout. 2008. Circumpolar thinning of Arctic sea ice following the 2007 record ice extent minimum. *Geophys. Res. Lett.,* **35**(22), L22502. (10.1029/2008GL035710.)

Grenfell, T.C. and D.K. Perovich. 2004. Seasonal and spatial evolution of albedo in a snow–ice–land–ocean environment. *J. Geophys. Res.,* **109**(C1), C1001. (10.1029/2003JC001866.)

Haas, C., A. Pfaffling, S. Hendricks, L. Rabenstein, J.-L. Etienne and I. Rigor. 2008. Reduced ice thickness in Arctic Transpolar Drift favors rapid ice retreat. *Geophys. Res. Lett.,* **35**(17), L17501. (10.1029/2008GL034457.)

Hanesiak, J.M., D.G. Barber, R.A. De Abreu and J.J. Yackel. 2001. Local and regional albedo observations of Arctic first-year sea ice during melt ponding. *J. Geophys. Res.,* **106**(C1), 1005–1016.

Kay, J.E., A. Gettelman, G. Stephens and C. O'Dell. 2008. The contribution of cloud and radiation anomalies to the 2007 Arctic sea ice extent minimum. *Geophys. Res. Lett.,* **35**(8), L08503. (10.1029/2008GL033451.)

Kwok, R., G.F. Cunningham, M. Wensnahan, I. Rigor, H.J. Zwally and D. Yi. 2009. Thinning and volume loss of the Arctic Ocean sea ice cover: 2003–2008. *J. Geophys. Res.,* **114**(C7), C07005. (10.1029/2009JC005312.)

Liu, J.P., J.A. Curry, W.B. Rossow, J.R. Key and X.J. Wang. 2005. Comparison of surface radiative flux data sets over the Arctic Ocean. *J. Geophys. Res.,* **110**(C2), C02015. (10.1029/2004JC002381.)

Markus, T., J.C. Stroeve and J. Miller. 2009. Recent changes in Arctic sea ice melt onset, freezeup, and melt season length. *J. Geophys. Res.,* **114**(C12), C12024. (10.1029/2009JC005436.)

Maslanik, J.A., C. Fowler, J. Stroeve, S. Drobot and H.J. Zwally. 2007. A younger, thinner Arctic ice cover: increased potential for rapid, extensive ice loss. *Geophys. Res. Lett.,* **34**(24), L24501. (10.1029/2007GL032043.)

Maykut, G.A. and M.G. McPhee. 1995. Solar heating of the Arctic mixed layer. *J. Geophys. Res.,* **100**(C12), 24,691–24,703.

Nghiem, S.V., I.G. Rigor, D.K. Perovich, P. Clemente-Colón, J.W. Weatherly and G. Neumann. 2007. Rapid reduction of Arctic perennial sea ice. *Geophys. Res. Lett.,* **34**(19), L19504. (10.1029/2007GL031138.)

Pegau, W.S. and C.A. Paulson. 2001. The albedo of Arctic leads in summer. *Ann. Glaciol.,* **33**, 221–224.

Perovich, D.K., T.C. Grenfell, B. Light and P.V. Hobbs. 2002. Seasonal evolution of the albedo of multiyear Arctic sea ice. *J. Geophys. Res.,* **107**(C10), 8044. (10.1029/2000JC000438.)

Perovich, D.K., B. Light, H. Eicken, K.F. Jones, K. Runciman and S.V. Nghiem. 2007a. Increasing solar heating of the Arctic Ocean and adjacent seas, 1979–2005: attribution and role in the ice-albedo feedback. *Geophys. Res. Lett.,* **34**(19), L19505. (10.1029/2007GL031480.)

Perovich, D.K., S.V. Nghiem, T. Markus and A.J. Schweiger. 2007b. Seasonal evolution and interannual variability of the local solar energy absorbed by the Arctic sea ice–ocean system. *J. Geophys. Res.,* **112**(C3), C03005. (10.1029/2006JC003558.)

Perovich, D.K., J.A. Richter-Menge, K.F. Jones and B. Light. 2008. Sunlight, water, and ice: extreme Arctic sea ice melt during the summer of 2007. *Geophys. Res. Lett.,* **35**(11), L11501. (10.1029/2008GL034007.)

Perovich, D.K. *and 8 others.* 2010. Arctic sea-ice melt in 2008 and the role of solar heating. *Ann. Glaciol.,* **51**(57) (see paper in this issue).

Polyakov, I., D. Walsh, I. Dmitrenko, R.L. Colony and L.A. Timokhov. 2003. Arctic Ocean variability derived from historical observations. *Geophys. Res. Lett.,* **30**(6), 1298. (10.1029/2002GL016441.)

Richter-Menge, J. 2009. The Arctic. *Bull. Am. Meteorol. Soc.* 90, Special issue, 51–5196.

Rigor, I.G. and J.M. Wallace. 2004. Variations in the age of Arctic sea-ice and summer sea-ice extent. *Geophys. Res. Lett.,* **31**(9), L09401. (10.1029/2004GL019492.)

Rothrock, D.A., D.B. Percival and M. Wensnahan. 2008. The decline in arctic sea-ice thickness: separating the spatial, annual, and interannual variability in a quarter century of submarine data. *J. Geophys. Res.,* **113**(C5), C05003. (10.1029/2007JC004252.)

Serreze, M.C., J.R. Key, J.E. Box, J.A. Maslanik and K. Steffen. 1998. A new monthly climatology of global radiation for the Arctic and comparisons with NCEP–NCAR reanalysis and ISCCP-C2 fields. *J. Climate,* **11**(2), 121–136.

Serreze, M.C., M.M. Holland and J. Stroeve. 2007. Perspectives on the Arctic's shrinking sea-ice cover. *Science,* **315**(5818), 1533–1536.

Shimada, K. *and 7 others*. 2006. Pacific Ocean inflow: influence on catastrophic reduction of sea ice cover in the Arctic Ocean. *Geophys. Res. Lett.,* **33**(8), L08065. (10.1029/2005GL025624.)

Smith, D.M. 1998. Recent increase in the length of the melt season of perennial Arctic sea ice. *Geophys. Res. Lett.,* **25**(5), 655–658.

Steele, M., W. Ermold and J. Zhang. 2008. Arctic Ocean surface warming trends over the past 100 years. *Geophys. Res. Lett.,* **35**(2), L02614. (10.1029/2007GL031651.)

Stroeve, J. *and 7 others*. 2008. Arctic sea ice extent plummets in 2007. *Eos,* **89**(2), 13–14

Walsh, J.E., W.L. Chapman and D.H. Portis. 2009. Arctic cloud fraction and radiative fluxes in atmospheric reanalyses. *J. Climate,* **22**(9), 2316–2334.

Woodgate, R.A., K. Aagaard and T.J. Weingartner. 2006. Interannual changes in the Bering Strait fluxes of volume, heat and freshwater between 1991 and 2004. *Geophys. Res. Lett.,* **33**(15), L15609. (10.1029/2006GL026931.)

https://doi.org/10.3189/172756411795931543 Published online by Cambridge University Press